

University of Groningen

An integrated simulation tool for analyzing the Operation and Interdependency of Natural Gas and Electric Power Systems

Pambour, Kwabena Addo; Erdener, Burcin Cakir; Bolado-Lavin, Ricardo; Dijkema, Gerhard

Published in:
 Pipeline Simulation Interest Group

IMPORTANT NOTE: You are advised to consult the publisher's version (publisher's PDF) if you wish to cite from it. Please check the document version below.

Document Version
 Publisher's PDF, also known as Version of record

Publication date:
 2016

[Link to publication in University of Groningen/UMCG research database](#)

Citation for published version (APA):

Pambour, K. A., Erdener, B. C., Bolado-Lavin, R., & Dijkema, G. (2016). An integrated simulation tool for analyzing the Operation and Interdependency of Natural Gas and Electric Power Systems. In Pipeline Simulation Interest Group

Copyright

Other than for strictly personal use, it is not permitted to download or to forward/distribute the text or part of it without the consent of the author(s) and/or copyright holder(s), unless the work is under an open content license (like Creative Commons).

Take-down policy

If you believe that this document breaches copyright please contact us providing details, and we will remove access to the work immediately and investigate your claim.

Downloaded from the University of Groningen/UMCG research database (Pure): <http://www.rug.nl/research/portal>. For technical reasons the number of authors shown on this cover page is limited to 10 maximum.

PSIG 1609

An integrated simulation tool for analyzing the Operation and Interdependency of Natural Gas and Electric Power Systems

Kwabena Addo Pambour^{a,*}, Burcin Cakir Erdener^b, Ricardo Bolado-Lavin^c, Gerard P. J. Dijkema^a

^a University of Groningen, Energy and Sustainability Research Institute Groningen (ESRIG), Groningen, The Netherlands

^b European Commission, Joint Research Centre, Institute for Energy and Transport, Ispra, Italy

^c European Commission, Joint Research Centre, Institute for Energy and Transport, Petten, The Netherlands

© Copyright 2016, PSIG, Inc.

This paper was prepared for presentation at the PSIG Annual Meeting held in Vancouver, British Columbia, 11 May - 13 May 2016.

This paper was selected for presentation by the PSIG Board of Directors following review of information contained in an abstract submitted by the author(s). The material, as presented, does not necessarily reflect any position of the Pipeline Simulation Interest Group, its officers, or members. Papers presented at PSIG meetings are subject to publication review by Editorial Committees of the Pipeline Simulation Interest Group. Electronic reproduction, distribution, or storage of any part of this paper for commercial purposes without the written consent of PSIG is prohibited. Permission to reproduce in print is restricted to an abstract of not more than 300 words; illustrations may not be copied. The abstract must contain conspicuous acknowledgment of where and by whom the paper was presented. Write Librarian, Pipeline Simulation Interest Group, 945 McKinney, Suite #106, Houston, TX 77002, USA - info@psig.org.

ABSTRACT

In this paper, we present an integrated simulation tool for analyzing the interdependency of natural gas and electric power systems in terms of security of energy supply. In the first part, we develop mathematical models for the individual systems. In part two, we identify the interconnections between both systems and propose a method for coupling the combined simulation model. Next, we develop the algorithm for solving the combined system and integrate this algorithm into a simulation software. Finally, we demonstrate the value of the software in a case study on a real world interconnected gas and electric power system of an European region.

NOMENCLATURE

EU: European Union
 CEI: Critical energy infrastructures
 CGS: City Gate Station
 GPP: Gas Fired Power Plant
 LNG: Liquefied Natural Gas
 PDE: Partial Differential Equation

TSO: Transmission System Operator
 UGS: Underground Gas Storage
A : incidence matrix
A : cross-sectional area
b : line charging susceptance
c : speed of sound
CV : Control Volume, calorific value
D : inner pipe diameter
e : Euler's number
F : residual vector
f : electric driver factor
g : gravitational acceleration
H : elevation
I : electric current
I_w : storage working inventory
J : Jacobi matrix
k : iteration step
k_c : constraint handling iteration step
K_i : participation factor
L : nodal load (vector)
L_{set} : load set point
L^{Elec} : gas offtake of power plants
L^{inj} : injection rate
L^{wdr} : withdrawal rate
l : pipe length
l_e : equivalent pipe length
LP : line pack
m : number of branches
n : number of nodes or buses
P : square pressure, active power
P_D : active power demand
P_D^{CS} : power demand of compressor stations
P_G : active power generation
P_G^{set} : active power generation set point
 ΔP : square pressure drop, power imbalance
p : gas pressure (vector)
 Δp : pressure drop

*corresponding author, Email: k.a.pambour@rug.nl

p_1 :	inlet pressure
p_2 :	outlet pressure
p_i :	inlet pressure
p_o :	outlet pressure
P_{set} :	pressure set point
P_{Loss} :	active power loss
p_m :	mean pressure
p_n :	pressure at reference conditions
POW_d :	driver power
POW_s :	shaft power
Q :	flow rate, reactive power
Q_{vol} :	volumetric flow rate
Q_{set} :	flow rate set point
$Q_{vol,set}$:	volumetric flow rate set point
Res :	residual
R :	gas constant, line resistance
R_f :	pipe resistance factor
R_i :	pipe inertia factor
t :	time
t_n :	time point
Δt :	time step
T :	temperature
T_n :	standard temperature
v :	gas velocity
V :	complex voltage
$ V $:	voltage magnitude
V_i :	nodal volume
X :	line reactance
x :	pipeline coordinate
\mathbf{x} :	solution vector
Δx :	pipe segment length
Y :	line admittance
\mathbf{Y}_{bus} :	bus admittance matrix
z :	height coordinate
Z :	compressibility factor, impedance
α :	inclination
δ :	voltage angle
ε :	residual tolerance
ζ :	resistance factor
η :	dynamic viscosity
η_{ad} :	adiabatic efficiency
η_m :	driver efficiency
η_T :	thermal efficiency
κ :	isentropic exponent
λ :	friction factor
Π :	pressure ratio
ϕ_{shift} :	transformer phase shift angle
ρ :	gas density

INTRODUCTION

The ongoing integration of renewable energy resources into the energy portfolio of the European Union is connected with an

increased interconnection between the different critical energy infrastructures (CEI). The interdependency between natural gas and electric power systems, for instance, is expected to grow in the near future. On the electric side, the demand for flexible backup power for intermittent renewable energy sources is increasing, which can be met by gas fired power plants (GPP) connected to the gas and electric grid, while on the gas side an increased use of electric power to operate facilities in the gas system can be observed (e.g. electric driven compressors, electric power supply to LNG Terminals etc.). Moreover, the present advancement in the Power-to-Gas technology will significantly contribute to the coupling of both systems. These trends suggest the need for simulation models to examine the depth and scope of these interdependencies, how they may affect the operation of both systems and how to proactively approach the bottlenecks that may emerge. Furthermore, developing combined gas and electricity models will also facilitate the development of Risk Assessment for this type of coupled networks.

In this paper, we present an integrated simulation tool, **SAInt** (**S**cenario **A**nalysis **I**nterface for Energy Systems), for analyzing the interdependency of gas and electric power systems in terms of security of energy supply, i.e. the uninterrupted supply of energy to its customers (e.g. commercial, residential, industrial customers, public services and power generation companies) particularly in case of difficult climatic conditions and in the event of disruptions [1].

The first part of the paper, focuses on developing the mathematical models for both systems. The second part, elaborates the interconnections between both systems and derives coupling equations for the combined system, followed by a description of the algorithm for solving the resulting system of equations. Finally, the capability of the simulation tool is demonstrated by applying it to a real world instance.

METHODOLOGY

The operation of gas and electric power systems is increasingly interdependent, due to an increased physical interconnection between the facilities installed in both systems. A change in one system may propagate to the other system and even back to the triggering system. For instance, an increase in power generation from a gas fired power plant, will cause the gas offtake from the gas grid to increase. This, in turn, may result in an increased power offtake of electric driven compressor stations to recover the pressure and line pack level in the area affected by the gas offtake. This additional power offtake, again, will trigger an increase in power generation which has to be balanced by the power generation units. This cycle may continue until an equilibrium state is reached.

The goal of a combined gas and power system study is to find for each time step a state of the coupled system, that satisfies the

physical equations describing the behavior of the gas and power system and the coupling equations describing the link between both systems, taking into account the controls and constraints imposed by the different facilities involved in the transport process.

The first challenge that arises, when modeling the coupled gas and power system is to find a simulation model that describes the dynamic behavior of the individual system appropriately. The dynamics in gas transport systems, for instance, are much slower than the one in power systems. Electricity travels almost instantaneously and cannot be stored economically in large quantities in current power systems¹ [2]. In case of a disruption, the response time of the power system is quite small and basically the transmission line flows satisfy the steady-state algebraic equations. On the contrary, natural gas pipeline flow is a much slower process, with gas velocities typically below 10 m/s (50 [ft/s]), resulting in a longer response time in case of a large fluctuation. In particular, high-pressure transmission pipelines have much slower dynamics due to the large sums of natural gas stored in the pipelines.

Considering the different characteristics of both systems, in this paper, we propose a transient model for the gas system and a steady-state AC- power flow model for the power system. We couple both models to a combined simulation model by defining coupling equations reflecting the physical interlink between both systems. In the following, we derive the gas and power system model independently. Next, we identify the interconnection between both systems and develop the coupling equations for the combined model.

GAS SYSTEM MODEL

In this section, we give a brief overview of the gas system model implemented in the simulation tool **SAInt**. Furthermore, we demonstrate the accuracy of the model by comparing simulation results for a well known sample network to results obtained with a commercial software. For a more detailed description of the gas model, we refer to PAMBOUR et al. [3].

The purpose of a gas transport system is to transport natural gas from remote production sites to demand areas, where gas is needed for heating, power generation or as a feed stock for industrial production. The transport of natural gas involves the use of different types of facilities, such as pipelines, compressor stations, regulator stations and valves. These facilities are supervised and controlled by Transmission System Operators (TSO), to ensure a safe, reliable and economical operation of the transport system.

A gas network is usually described by a directed graph composed of nodes and branches. Facilities with an inlet, outlet

and flow direction are modeled as branches, while connection points between these branches as well as entry and exit stations are represented by nodes. Branches, in turn, can be distinguished between active and passive branches. Active branches represent controlled facilities, which can change their state or control during operation, such as compressor stations, regulator stations and valves (s. Table 2), while passive branches, such as pipelines and resistors represent facilities or components which state is fully described by the physical equations (s. Table 1). The topology of the network can be described by the following node-branch incidence matrix.

$$\mathbf{A} = [a_{ij}]^{n \times m} \quad (1)$$

with

$$a_{ij} = \begin{cases} +1, & \text{node } i \text{ is outlet of branch } j \\ -1, & \text{node } i \text{ is inlet of branch } j \\ 0, & \text{node } i \text{ and branch } j \text{ are not connected} \end{cases}$$

where n is the number of nodes and m the number of branches in the network.

The gas flow in transport pipelines is inherently dynamic. Supply and demand are constantly changing and the reaction of the system to these changes are relatively slow, due to the small flow velocities (typically below 10 [m/s], approx. 50 [ft/s]) and the large volume of gas stored in transport pipelines.

The dynamic behavior of a gas system is predominately determined by the gas flow in pipelines. In general, a gas pipeline has four basic properties, namely, capacity (i.e. the ability to store a certain volume of gas, which depends on the geometric volume and maximum pipeline pressure), resistance (i.e. force acting opposite to the gas flow direction, caused by friction between gas and the inner walls of the pipeline), inertia (force acting opposite to the gas flow acceleration) and gravity (gravitational force acting on the gas volume in sloped pipelines). Capacity and resistance are the predominant properties, while in most cases gravity and inertia play a secondary role. The pipe elements in a gas network can be segmented into a number of pipe sections, assuming each section inherits a proportional fraction of the properties of the original pipeline[4]. Fig. 1 demonstrates this for a cross section of a pipeline. As can be seen, the volumes of the pipelines are equally distributed and assigned to the inlet and outlet nodes, respectively. According to the mass conservation law, the gas density ρ_i in a nodal control volume V_i may change in time, if there is an imbalance between gas inflow and outflow to V_i . If we assume isothermal flow conditions, the mass conservation law can be expressed by the following integral form of the continuity equation:

$$\frac{V_i}{\rho_n c^2} \frac{dp_i}{dt} = \sum_{j=1}^k a_{ij} Q_{ij} - L_i \quad (4)$$

¹with the only exception of hydraulic pumping power stations, whose availability is very much limited in a significant number of countries

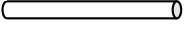

Element	Function	Equations [3]
pipe 	transport of natural gas from point a to b, short term gas storage	$\Delta P^{n+1} = R_f \cdot Q^{n+1} Q^{n+1} + R_i \cdot (Q^{n+1} - Q^n) \quad (2)$ $\Delta P^{n+1} = p_1^{2,n+1} - p_2^{2,n+1} e^s, \quad R_i = \frac{2\rho_n l_e p_m}{\Delta t A}$ $s = \frac{2g(H_2 - H_1)}{c^2}, \quad R_f = \frac{16\lambda \rho_n^2 c^2 l_e}{\pi^2 D^5}$ $l_e = \begin{cases} l, & H_1 = H_2 \\ \frac{e^s - 1}{s} l, & H_1 \neq H_2 \end{cases}, \quad p_m = \frac{2}{3} \frac{p_1^2 + p_1 p_2 + p_2^2}{p_1 + p_2}$
resistor 	passive devices that cause a local pressure drop (e.g. meters, inlet piping, coolers, heaters, scrubbers etc.)	$p_1 - p_2 = \zeta \frac{\rho}{2} v v \quad (3)$

Table 1: Basic passive elements in a gas network model

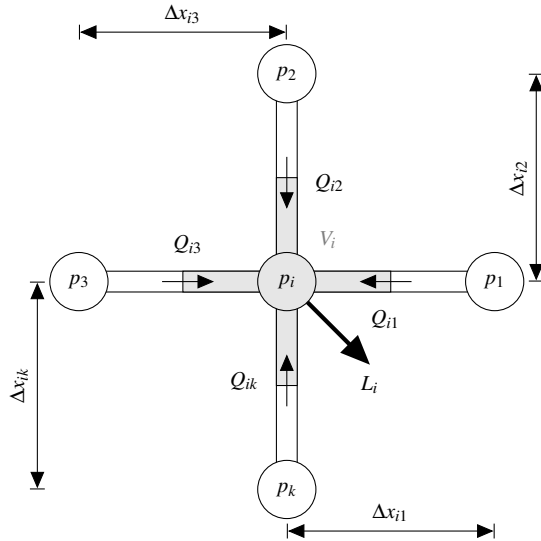


Figure 1: Law of conservation of mass applied to a nodal control volume in cross section of a pipeline network

with

$$c^2 = \frac{p}{\rho} = ZRT, \quad V_i = \frac{\pi}{8} \sum_{j=1}^k D_{ij}^2 \Delta x_{ij}$$

where Q_{ij} is the flow rate from node i to j at reference conditions, ρ_n the gas density at reference conditions, L_i the external load on node i , c the isothermal speed of sound, Z the gas compressibility factor, R the specific gas constant, T the gas temperature, Δx_{ij} and D_{ij} the length and diameter of pipe segment (ij), respectively. The continuity equation can be expressed for each nodal control volume in the network, thus, we obtain (n)

set of equations with $2n + m$ unknown state variables (p_i , $Q_{i,j}$ and L_i). If we perform an implicit time integration on this set of equations for a time step $\Delta t = t_{n+1} - t_n$ and order the equation in terms of known variables at time t_n and t_{n+1} (right hand side) and unknown variables at time t_{n+1} (left hand side), we obtain the following set of linear finite difference equations for the total network:

$$\Phi p^{n+1} - \mathbf{A} Q^{n+1} = \Phi p^n - 0.5 (L^n + L^{n+1}) \quad (5)$$

where Q and L are the vectors of branch flows and nodal loads, respectively, and Φ the following diagonal matrix, describing the pressure coefficients ϕ_i :

$$\Phi = \text{diag}\{\phi_1, \phi_2, \dots, \phi_n\}, \quad \phi_i = \frac{V_i}{\rho_n c^2 \Delta t} \quad (6)$$

In order to close and solve eq. (5) for the entire network including non-pipe facilities, $n + m$ additional independent equations are needed (i.e. one equation for each branch and each node in the network), which correlate the state variables p_i , Q_{ij} and L_i . These equations are provided by the pressure drop equation for each pipe section and the equations describing the control modes of non-pipe facilities. Tables 2, 3 & 4 give an overview of the implemented control modes, constraints and their corresponding linearized equations for non-pipe facilities modeled as active branches and nodes, respectively.

The pressure drop equation for a pipe section is derived from the law of conservation of momentum as shown in Fig. 2, where the different forces acting on a control volume in a pipe section are illustrated. The resulting momentum equation yields:

$$\underbrace{\frac{\partial(\rho v)}{\partial t}}_{\text{inertia}} + \underbrace{\frac{\partial(\rho v^2)}{\partial x}}_{\text{convective term}} + \underbrace{\frac{\partial p}{\partial x}}_{\text{pressure}} + \underbrace{\frac{\lambda \rho v |v|}{2D}}_{\text{friction}} + \underbrace{\rho g \sin \alpha}_{\text{gravity}} = 0 \quad (7)$$

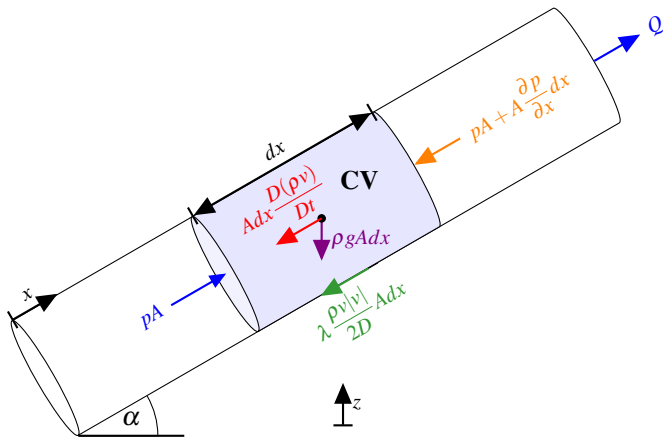


Figure 2: Forces acting on a control volume in a general gas pipeline

where v is the gas flow velocity and λ the Darcy friction factor. Eq. 7 can be reduced to the following non-linear partial differential equation (PDE), if we assume isothermal flow conditions and neglect the convective term².

$$\frac{\partial p}{\partial x} = -\frac{\rho_n}{A} \frac{\partial Q}{\partial t} - \frac{\lambda \rho_n^2 c^2}{2DA^2 p} |Q|Q - \frac{g \sin \alpha}{c^2} p \quad (8)$$

where A denotes the cross-sectional area of the pipe section. Eq. 8 can be discretized using an implicit finite difference scheme as shown in Table 1, where l denotes the length, H_1 and H_2 the inlet and outlet elevation of a pipe segment, respectively. In sum, the system of equations describing the behavior of the gas system can be expressed by the following linearized matrix equation:

$$\begin{pmatrix} \Phi & -A & \mathbf{I} \\ \mathbf{C}_p & \mathbf{C}_Q & \mathbf{0} \\ \mathbf{K}_p & \mathbf{K}_Q & \mathbf{K}_L \end{pmatrix} \begin{pmatrix} p^{n+1} \\ Q^{n+1} \\ L^{n+1} \end{pmatrix} = \begin{pmatrix} \Phi p^n \\ D \\ S \end{pmatrix} \quad (9)$$

where the first row describes the continuity equation, the second row the linearized equation for passive and active branches (s. Table 1, 2 & 4) and the third row the equations for the control mode of entry, exit stations, LNG terminals and underground gas storage facilities (s. Table 3). Eq. 9 is solved iteratively for each simulation time step t_{n+1} using the initial state t_0 or the solution of a preceding time step t_n as an initial guess for the iterative linearization. We adapted the linearization methods presented by van der Hoeven [5] for the steady state to the transient case. The algorithm is detailed in [3].

MODEL BENCHMARKING

In the following, we benchmark the accuracy of the presented gas model against results from the commercial software SI-

²this term is negligible compared to the other terms in the momentum equation, since the flow velocity in pipelines is much smaller than the speed of sound [3]

MONE for a sample network adapted from [6]. The data of the network topology, gas and pipe properties and steady state boundary conditions are given in Tables 8 and 9. In the first step, we run a steady state simulation to obtain an initial state of the network, which we then use in a second step to compute a dynamic simulation over 24 hours, using the load profile shown in Figure 18, which we multiply with the steady state load for each demand node. Figures 3 and 4 show the steady state solution, while Figure 5 illustrates the results for the dynamic simulation. As can be seen, the results obtained with SAInt are very similar to the SIMONE results, which confirms the accuracy of the simulation model. The comparison of the steady state results obtained with SAInt (s. Figure 3) and SIMONE (s. Figure 4) shows small deviations (< 0.2 [bar], 2.9 [psi]) in the nodal pressure and compressor flow rate (< 2 [k m^3/h], 1.62 [mm sfcfd]) in the area around compressor station Co3. Similar observations can be made for the time plots for the dynamic simulation (s. Figure 5). The shape of the time plots for the gas supply in the source node (s. Figure 5 a)) and the nodal pressure for three selected nodes (s. Figure 5 b) c) and d)) obtained with SAInt and SIMONE are very similar, however, small deviations (< 0.2 [bar], 2.9 [psi]) can be observed for the last five simulation hours. Discrepancies for the transient model in other nodes are in the same range as the ones shown here. We consider these discrepancies (below 0.5%) as quite good results.

POWER SYSTEM MODEL

After presenting the model for the gas system, in this section we elaborate the model implemented for the power system. In the first part, we give an overview of the different elements involved in the operation of a power system, their function and constraints. Finally, we develop the system of equations describing the steady state power flow in power systems.

An electric power system can be divided into three subsystems operating at different voltage levels, namely, the generation (11-35[kV]), transmission (usually above 110[kV]) and distribution system (11k- 400 [V] or 230 [V])³. The generation system produces electricity by converting primary energy sources (e.g. fossil fuels, wind, hydro etc.) to electric energy, using synchronous turbo generators, which are driven by gas, steam, water or wind turbines. The generating units inject Alternating Currents (AC) to a 3-phase transmission system at a constant voltage magnitude ($|V|$) and frequency (f) (usually 50 [Hz]). Voltage magnitude and frequency are typically controlled by a designated Automatic Generation Control System (AGC) [7].

In order to reduce the power losses incurred during transportation ($\cong I^2 \cdot R$), the output voltages of generation units are usually increased to transmission system level using step up transformers. The transmission system provides a network of in-

³the primary distribution system typically starts at 6.6 [kV], 3.3 [kV] or 11 [kV] and the secondary distribution system is 230 or 400 [kV]

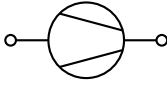
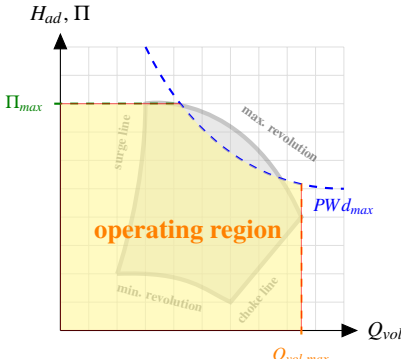
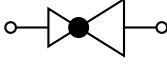

Facility	Function	Control Modes	Constraints	Envelope
Compressor Station 	compensates the pressure and head losses due to friction and heat transfer by increasing the gas pressure	inlet pressure ($p_{i,set}$) outlet pressure ($p_{o,set}$) pressure ratio (Π_{set}) pressure difference (Δp_{set}) flow rate (Q_{set}) volumetric flow ($Q_{vol,set}$) shaft power ($PW_{s,set}$) driver power ($PW_{d,set}$) driver fuel ($Q_{f,set}$) closed (<i>OFF</i>) bypass (<i>BP</i>)	<u>internal hard limits:</u> $p_o \geq p_i$ & $Q \geq 0$ <u>user defined limits:</u> max. outlet pressure ($p_{o,max}$) min. inlet pressure ($p_{i,min}$) max. volumetric flow ($Q_{vol,max}$) max. flow rate (Q_{max}) max. pressure Ratio (Π_{max}) max. driver power ($PW_{d,max}$)	
Regulator Station 	reduces the upstream pressure to a lower downstream pressure and/or regulates the gas flow rate	inlet pressure ($p_{i,set}$) outlet pressure ($p_{o,set}$) pressure difference (Δp_{set}) flow rate (Q_{set}) volumetric flow ($Q_{vol,set}$) closed (<i>OFF</i>) bypass (<i>BP</i>)	<u>internal hard limits:</u> $p_i \geq p_o$ & $Q \geq 0$ <u>user defined limits:</u> max. outlet pressure ($p_{o,max}$) min. inlet pressure ($p_{i,min}$) max. volumetric flow ($Q_{vol,max}$) max. flow rate (Q_{max})	-
Valve Station 	interrupts the gas flow and shuts-off sections of the gas network for maintenance or safety reasons	closed (<i>OFF</i>) opened (<i>BP</i>)	<u>internal hard limit:</u> $V \leq 60$ [m/s] <u>user defined limits:</u> max. flow velocity (V_{max})	-

Table 2: Overview of available control modes and constraints settings for active elements

terconnected lines and substations to enable a safe and reliable transport of electric power to large customers directly served from the transmission grid and to smaller customers supplied through the local distribution system. The distribution system is typically operated at lower voltage levels, thus, the voltage level of the transmission system is reduced by step down transformers installed at substations connected to the distribution system. In this paper, we focus primarily on the high voltage electric transmission system, which is the most crucial subsystem in the power supply chain.

Similar to a gas network, a power transmission system can be described by a directed graph consisting of nodes and branches, where each branch represent a transmission line or a transformer and each node a connection point between two or more electrical components, also referred to as bus. At some of the buses power is injected into the network, while at others power

is consumed by system loads. In contrast to gas systems, power systems are predominantly in steady state operation or in a state that could with sufficient accuracy be regarded as steady state [8]. Thus, the 3-phase transmission system is typically modeled as a balanced per phase equivalent system using linear models for the elements involved in the transport process. A transmission line, for instance, can be described by an equivalent π -circuit as depicted in Table 5, which considers the basic properties of an actual transmission line, such as line resistance R_{ij} , line reactance X_{ij} and line charging susceptance b_{ij} . Using these properties the complex inlet and outlet bus voltages V_i and V_j can be related to their corresponding complex current injections I_{ij} and I_{ji} through the branch admittance matrix Y_{br} as shown in eq. (10) in Table 5. A similar branch admittance matrix can be expressed for in-phase and phase shifting transformers as listed in eq. (11) in Table 5.

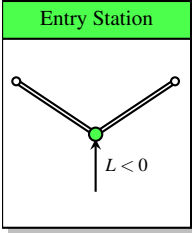
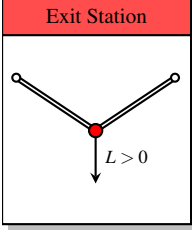
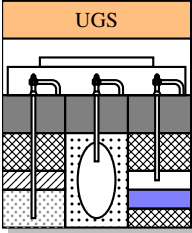
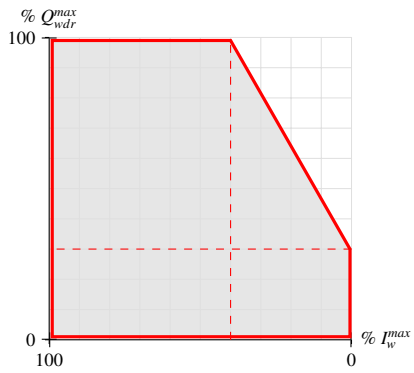
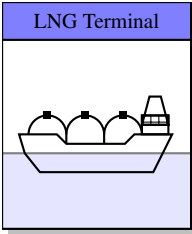
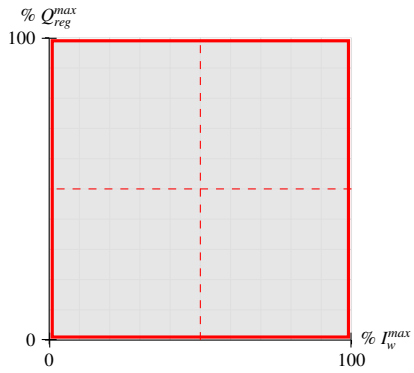
Facility	Control Modes	Constraints	Envelope
	<p>pressure (p_{set}) inflow (Q_{set})</p>	<p><u>internal hard limits:</u> $L \leq 0$</p> <p><u>user defined limits:</u> min. supply flow (Q_{min}) max. supply flow (Q_{max}) min. supply pressure (p_{min}) max. supply pressure (p_{max})</p>	<p>-</p>
	<p>pressure (p_{set}) outflow (Q_{set})</p>	<p><u>internal hard limits:</u> $L \geq 0$</p> <p><u>user defined limits:</u> min. delivery flow (Q_{min}) max. delivery flow (Q_{max}) min. delivery pressure (p_{min}) max. delivery pressure (p_{max})</p>	<p>-</p>
	<p>pressure (p_{set}) withdrawal/injection rate (Q_{set}) initial working inventory (INV) withdrawal state (WDR) injection state (INJ)</p>	<p><u>internal hard limits:</u> $L^{wdr} \leq 0$ & $L^{inj} \geq 0$</p> <p><u>user defined hard limits:</u> max. working inventory ($I_{w,max}$) max. withdrawal rate ($Q_{wdr,max}$) max. injection rate ($Q_{inj,max}$)</p> <p><u>user defined limits:</u> max. supply pressure ($p_{wdr,max}$) min. offtake pressure ($p_{inj,min}$)</p>	
	<p>pressure (p_{set}) regasification rate (Q_{set}) initial working inventory (INV) arriving vessel size ($VESSEL$)</p>	<p><u>internal hard limits:</u> $L \leq 0$</p> <p><u>user defined hard limits:</u> max. working inventory ($I_{w,max}$) max. regasification rate ($Q_{reg,max}$)</p> <p><u>user defined limits:</u> max. supply pressure ($p_{reg,max}$)</p>	

Table 3: Overview of available control modes and constraints settings for non-pipe facilities modeled as nodes

Control Mode	Equation	Coefficients $c_1 \cdot p_1 + c_2 \cdot p_2 + c_3 \cdot Q = d$
inlet pressure ($p_{i,set}$)	$p_i = p_{i,set}$	$c_1 = 1, c_2 = 0, c_3 = 0, d = p_{i,set}$
outlet pressure ($p_{o,set}$)	$p_o = p_{o,set}$	$c_1 = 0, c_2 = 1, c_3 = 0, d = p_{o,set}$
pressure ratio (Π_{set})	$\frac{p_o}{p_i} = \Pi_{set}$	$c_1 = -\Pi_{set}, c_2 = 1,$ $c_3 = 0, d = 0$
pressure difference (Δp_{set})	$p_o - p_i = \Delta p_{set}$	$c_1 = -1, c_2 = 1,$ $c_3 = 0, d = \Delta p_{set}$
flow rate (Q_{set})	$Q = Q_{set}$	$c_1 = 0, c_2 = 0, c_3 = 1, d = Q_{set}$
volumetric flow ($Q_{vol,set}$)	$Q = \frac{p_i}{Z_i T_i R \rho_n} Q_{vol,set}$	$c_1 = -\frac{Q_{vol,set}}{Z_i T_i R \rho_n}, c_2 = 0,$ $c_3 = 1, d = 0$
shaft power ($PW_{s,set}$)	$PW_{s,set} = \frac{K_i Q}{c_\kappa} [\Pi^{c_\kappa} - 1]$ $K_i = \frac{Z_i T_i R \rho_n}{\eta_{ad}}, \Pi = \frac{p_o}{p_i}, c_\kappa = \frac{\kappa - 1}{\kappa}$	$c_1 = -\frac{K_i Q}{p_i} \Pi^{c_\kappa}, c_2 = \frac{K_i Q}{p_o} \Pi^{c_\kappa},$ $c_3 = \frac{K_i}{c_\kappa} [\Pi^{c_\kappa} - 1], d = PW_{s,set}$
driver power ($PW_{d,set}$)	$PW_{d,set} = \frac{K_i Q}{c_\kappa} [\Pi^{c_\kappa} - 1]$ $K_i = \frac{Z_i T_i R \rho_n}{\eta_{ad} \eta_m}, \Pi = \frac{p_o}{p_i}, c_\kappa = \frac{\kappa - 1}{\kappa}$	$c_1 = -\frac{K_i Q}{p_i} \Pi^{c_\kappa}, c_2 = \frac{K_i Q}{p_o} \Pi^{c_\kappa},$ $c_3 = \frac{K_i}{c_\kappa} [\Pi^{c_\kappa} - 1], d = PW_{d,set}$
bypass (BP)	$p_i = p_o$	$c_1 = -1, c_2 = 1, c_3 = 0, d = 0$
off (OFF)	$Q = 0$	$c_1 = 0, c_2 = 0, c_3 = 1, d = 0$

Table 4: Control modes for non-pipe facilities and their mathematical implementation

For the total network, a bus admittance matrix \mathbf{Y}_{bus} containing the elements of the individual branch admittance matrices can be expressed as follows:

$$\mathbf{I} = \mathbf{Y}_{bus} \mathbf{V} \quad (12)$$

where \mathbf{V} and \mathbf{I} denote the vectors of complex voltages and currents at each bus, respectively.

The in- and outflow of electric power to the power system is modeled by generation units, loads, shunt capacitors and reactors connected to the buses of the power system. Table 6

shows a list of these components, their function and constraints. The steady state analysis of a power system involves the determination of the voltage magnitudes $|V_i|$, voltage angles $|\delta_i|$, active power P_i and reactive power Q_i supply at each bus i , considering the constraints imposed by the different facilities and components in the power system. These state variables are computed from the power flow balance equation, derived from Kirchhoff's Current Law (KCL) applied to each bus. The power balance equation for a bus i yields the following two non-linear

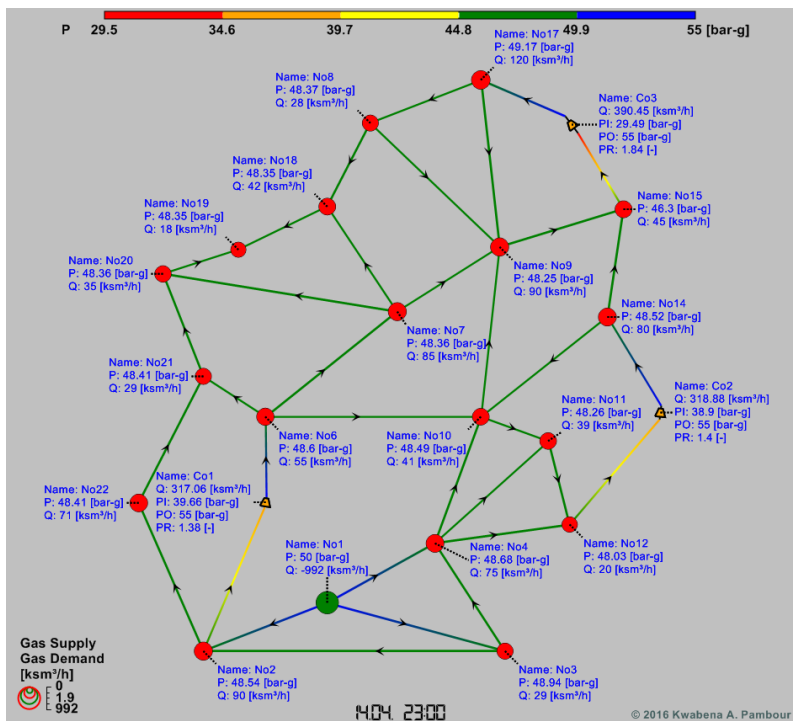


Figure 3: Steady state solution for the reference network obtained with SAInt

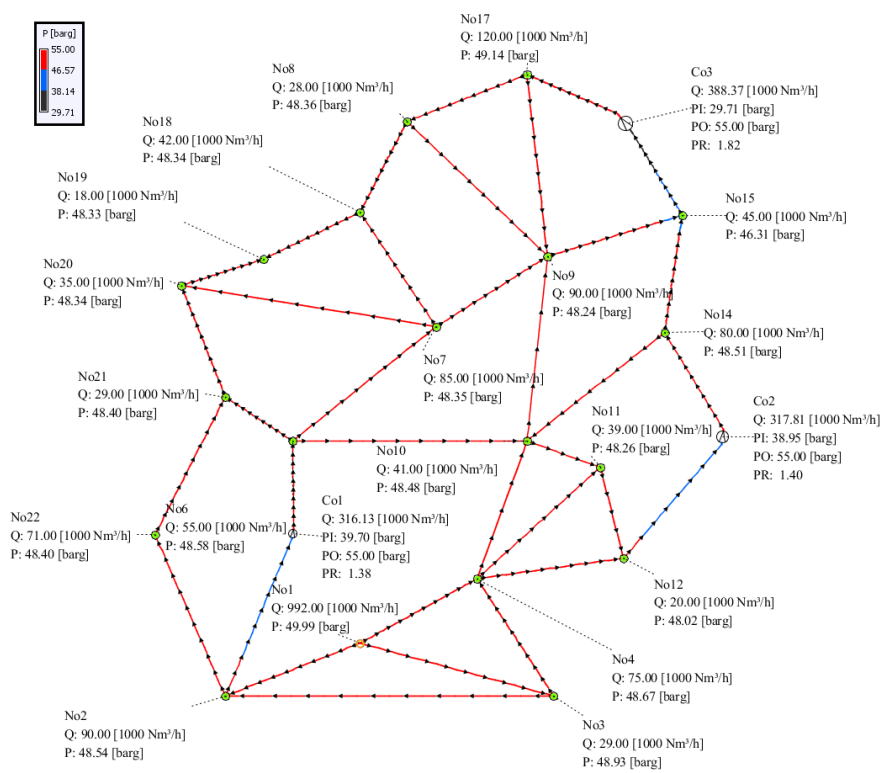


Figure 4: Steady state solution for the reference network obtained with SIMONE

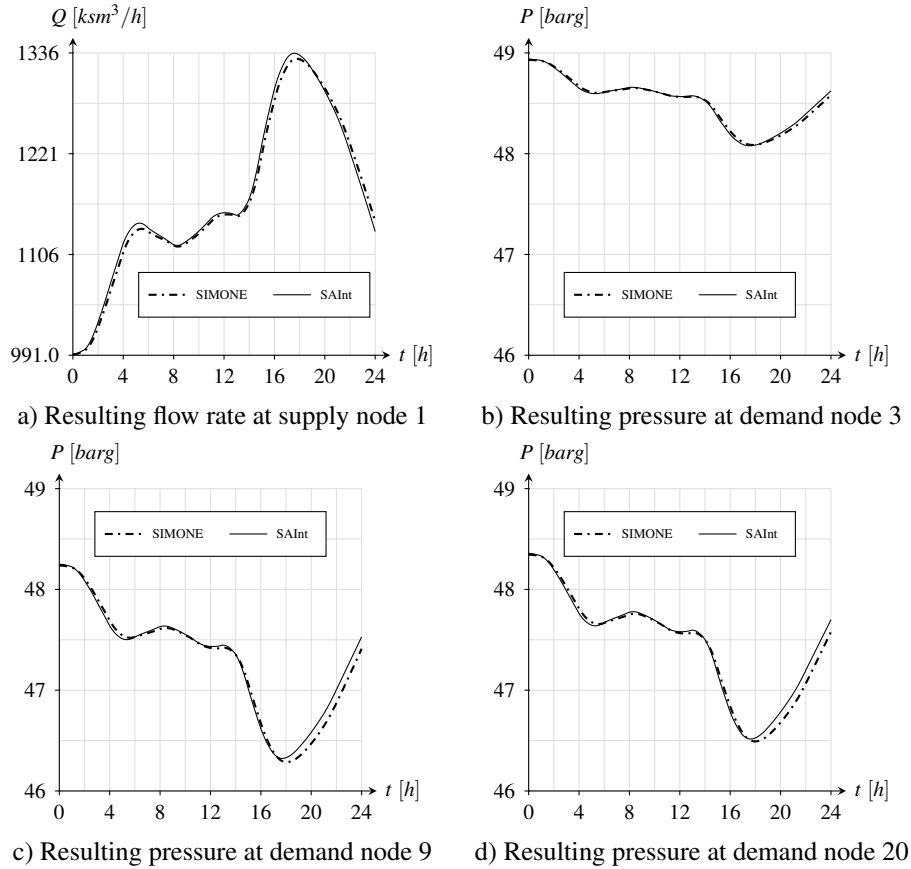


Figure 5: Comparison of simulation results for the reference network obtained with SAInt and SIMONE

equations for the active and reactive power balance:

$$P_i(\delta, |V|) = \sum_{j=1}^n |V_i||V_j||Y_{ij}|\cos(\delta_i - \delta_j - \theta_{ij}) \quad (13)$$

$$Q_i(\delta, |V|) = \sum_{j=1}^n |V_i||V_j||Y_{ij}|\sin(\delta_i - \delta_j - \theta_{ij}) \quad (14)$$

$$P_{G,i} - P_{D,i} - P_i(\delta, |V|) = 0 \quad (15)$$

$$Q_{G,i} - Q_{D,i} - Q_i(\delta, |V|) = 0 \quad (16)$$

where $P_{G,i}$, $Q_{G,i}$ are active and reactive power generation at bus i , respectively, $P_{D,i}$, $Q_{D,i}$ active and reactive power demanded at bus i , respectively, and $Y_{ij} = |Y_{ij}|(\cos(\theta_{ij}) + j\sin(\theta_{ij}))$ the elements of the bus admittance matrix describing the branch connection between bus i and any connected bus j . The solution of the power flow equations (13 - 16) requires additional boundary conditions, which are provided by the set points for generation units and loads. In the traditional power flow analysis, each bus is classified depending on the prescribed boundary conditions into the following three bus types:

1. Slack-Bus (Reference Bus):

Voltage magnitude $|V|$ and voltage angle δ are specified

and active power P and reactive power Q are computed. A slack bus is usually connected to a generation unit with terminal voltage control. At least one slack bus is needed as a voltage angle reference and also for balancing the active power losses not covered by other generation units.

2. PV-Bus (Generation Bus):

Active power P and voltage magnitude $|V|$ are prescribed and voltage angle δ and reactive power Q are computed. Buses connected to generation units with terminal voltage control are specified as PV-Buses. If the reactive power limit of a PV-Bus is violated during computation the PV bus is changed to a PQ-Bus and the reactive power is set to the next closest feasible working point.

3. PQ-Bus (Load Bus):

Active power P and reactive power Q are prescribed and voltage magnitude $|V|$ and voltage angle δ are computed. Buses with purely load connections are usually classified as PQ-Buses.

In a real power system, a single slack bus, that balances the active power of the total system does not exist. Thus, to model the power generation and the balancing of the power system more

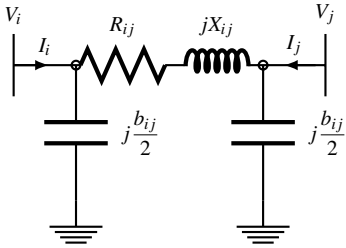
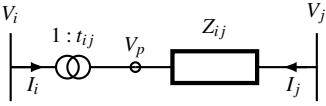
Facility	Equations	Constraints
<p>Transmission Line (π-Model)</p> 	$\begin{bmatrix} I_i \\ I_j \end{bmatrix} = \begin{bmatrix} (y_{ij} + \frac{b_{ij}}{2}) & -y_{ij} \\ -y_{ij} & (y_{ij} + \frac{b_{ij}}{2}) \end{bmatrix} \begin{bmatrix} V_i \\ V_j \end{bmatrix} \quad (10)$ <p>with</p> $V_i = V_i e^{j\delta_i}, \quad V_j = V_j e^{j\delta_j}, \quad y_{ij} = \frac{1}{R_{ij} + jX_{ij}}$	<p>flow of active and reactive power is limited by thermal capability of the transmission line</p>
<p>Transformer & Phase Shifter</p> 	$\begin{bmatrix} I_i \\ I_j \end{bmatrix} = \begin{bmatrix} a_{ij}^2 y_{ij} & -t_{ij}^* y_{ij} \\ -t_{ij} y_{ij} & y_{ij} \end{bmatrix} \begin{bmatrix} V_i \\ V_j \end{bmatrix} \quad (11)$ <p>with</p> $a_{ij} = \frac{ V_p }{ V_i }, \quad t_{ij} = a_{ij} e^{j\phi_{shift}}, \quad y_{ij} = \frac{1}{Z_{ij}}$	<p>heating limits</p>

Table 5: Basic elements in an electric network model

realistically, we introduce the concept of distributed slack bus generation discussed in [9, 10, 11], which enables the balancing of the power system by regulating the active power output of a selected number of generation units. For each generation unit, we specify an active power generation set point $P_{G,i}^{set}$ and a participation factor K_i , describing the flexibility of the generation unit to regulate a fraction of the required additional generation ΔP for balancing the power system. The additional generation can be expressed as follows:

$$\Delta P = \sum_{i=1}^n P_{G,i}^{set} - P_{D,i} - P_{Loss} \quad (17)$$

where P_{Loss} is the total power loss of the power system. The active power balance equation (13) can be modified as follows, while the reactive power balance equation (16) remain unchanged:

$$P_{G,i}^{set} + K_i \cdot \Delta P - P_{D,i} - P_i(\delta, |V|) = 0 \quad (18)$$

$$\sum_{i=1}^n K_i = 1 \quad (19)$$

The resulting system of non-linear power flow equations is solved iteratively using a Newton-Raphson approach:

$$\mathbf{J}(\mathbf{x}^k) \cdot \Delta \mathbf{x} = -\mathbf{F}(\mathbf{x}^k) \quad (20)$$

$$\mathbf{x}^{k+1} = \mathbf{x}^k + \Delta \mathbf{x} \quad (21)$$

where \mathbf{J} is the Jacobi matrix, \mathbf{F} residual vector and $\mathbf{x} = [\delta, |V|, \Delta P]^T$ the solution vector. The algorithm for solving eq. (16, 18, 20, 21) is detailed in [7, 8, 12].

INTERDEPENDENCY OF GAS AND ELECTRIC POWER SYSTEMS

Gas and electric power systems are physically interconnected at a number of facilities. The most significant interconnections between both systems are as follows:

1. Gas demand for power generation at gas fired power plants connected to the gas and electric power system. The gas offtake for power generation can be expressed as follows:

$$L_i^{Elec} = \frac{P_{G,i}^{set} + K_i \cdot \Delta P}{\eta_T \cdot CV} \quad (22)$$

where η_T is the thermal efficiency of the power plant and CV the calorific value of the fuel gas extracted from the pipeline.

2. Electric power demand for electric driven compressors installed in gas compressor stations and underground storage facilities. The electric power consumed by the compressor station can be described by the following expression describing the driver power:

$$P_{D,i}^{CS} = f \frac{\kappa}{\kappa - 1} \frac{Z_1 T_1 R \rho_n Q}{\eta_{ad} \eta_m} \left[\frac{p_2}{p_1} \frac{\kappa - 1}{\kappa} - 1 \right] \quad (23)$$

where f is a factor describing the fraction of total driver power provided by electric drivers, η_{ad} the average adiabatic efficiency of the compressors, η_m the average mechanical efficiency of the installed drivers, p_2 the outlet

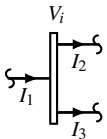
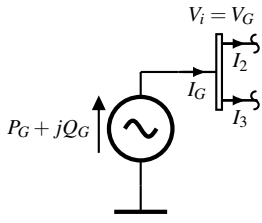
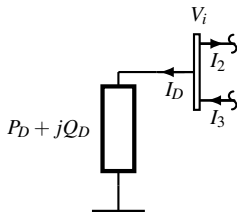
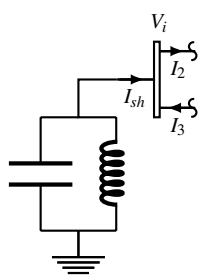
Facility	Function	Constraints
<p>Bus</p> 	<p>connection point between transmission lines, transformers, loads, capacitors, reactors,</p>	
<p>Generation</p> 	<p>injects electric power into the power system, by converting primary energy sources (oil, gas, coal, wind, hydro etc.) to electric energy; bus voltage V_i and frequency f_i at buses connected to generation units are typically controlled at a specific set point V_G, f_G</p>	<p>upper and lower limit on reactive power Q_G and active power P_G injection restricted by reactive power capability curve of the generation unit</p> $P_{G,min} \leq P_G \leq P_{G,max}$ <p style="text-align: center;">&</p> $Q_{G,min} \leq Q_G \leq Q_{G,max}$ <p>(i.e. operating region is restricted by field current heating limit, stator current heating limit, end region heating limit)</p>
<p>Load</p> 	<p>represents consumption of electric power by large customers directly served from the transmission grid or the total power consumption from the local distribution grid connected to the transmission system at the respective substation</p>	<p>upper and lower limits on voltage magnitude</p> $ V_{min} \leq V \leq V_{max} $
<p>Shunt Capacitor/Reactor</p> 	<p>shunt reactors are placed locally to control the steady state over-voltages at buses under light load conditions, while shunt capacitors are used to boost a bus voltage in a stressed system</p>	

Table 6: Basic components in an electric network model

pressure, p_1 , Z_1 , T_1 the inlet pressure, compressibility factor, temperature, respectively, R the gas constant, κ the isentropic exponent.

- Power supply to LNG Terminals for operating LNG tanks and low and high pressure pumps. We capture this interaction by assuming a linear relation between the regasifica-

tion rate L^{reg} and the power consumption of the terminal:

$$P_{D,i}^{LNG} = P_{D,i}^{0,LNG} + c \cdot L_i^{reg} \quad (24)$$

where $P_{D,i}^{0,LNG}$ is the fixed power supply to the LNG Terminal, c the coefficient of the flow rate dependent power supply.

The coupling of the gas and power system is established through the developed coupling equations. If we integrate these equations into the developed gas and power system model, we obtain the following modified set of equations describing the combined gas and electric power system.

$$\begin{pmatrix} \Phi & -\mathbf{A} & \mathbf{I} \\ \mathbf{C}_p & \mathbf{C}_Q & \mathbf{0} \\ \mathbf{K}_p & \mathbf{K}_Q & \mathbf{K}_L \end{pmatrix} \begin{pmatrix} p^{n+1} \\ Q^{n+1} \\ L^{n+1} \end{pmatrix} = \begin{pmatrix} \Phi p^n - L^{Elec} \\ D \\ S \end{pmatrix} \quad (25)$$

$$P_{G,i}^{set} + K_i \cdot \Delta P - P_{D,i} - P_{D,i}^{LNG} - P_{D,i}^{CS} - P_i(\delta, |V|) = 0 \quad (26)$$

The algorithm for solving the combined simulation model is illustrated in the flow diagram in Figure 6. The simulation starts from an initial state, which can be obtained from a combined steady state computation or any other terminal state of a (combined) transient computation. The solution for each simulation time step is obtained iteratively by solving the system of equations for both systems (eq. (20 & 25)) separately and in parallel using multiple threads. The boundary conditions for both models are updated each iteration step using the coupling equations for the interconnected facilities (eq. (22, 23 & 24)). If the solution for a time step violates any constraints from Tables 2, 3, 5 & 6 a constraint and control handling algorithm, which tries to find a feasible working point for the affected facility, is invoked and the time integration is repeated with the new settings.

MODEL APPLICATION

The models presented in this paper were implemented in **SAInt** (Scenario Analysis Interface for Energy Systems), an integrated simulation software for performing steady state and dynamic simulations on gas and electric power systems. The software was developed with the objective of analyzing the operation and interdependency of critical energy infrastructures in terms of security of energy supply. **SAInt** was developed in MS Visual Studio .NET using the object oriented programming languages VB.NET, C# and C++ and can be used as a standalone gas simulator, standalone power system simulator or as a combined gas and power system simulator. It is divided into two separate modules, namely, **SAInt-API** (Application Programming Interface) and **SAInt-GUI** (Graphical User Interface). The API is the main library of the software and contains all solvers and classes for instantiating the different objects comprising a gas and electric power system. The API is independent of the GUI and can be used separately in any other .NET environment (e.g. MS Excel, IronPython etc.). **SAInt-GUI** is the graphical interface, which enables a visual communication between the API and the user. The GUI uses the classes and solvers from the API to perform the simulation tasks requested by the user. To extend the functionality of the software, the API has been linked with MATLAB using the Matlab COM Automation Server. This enables the API to communicate with the Matlab Command Window and execute Matlab

scripts. This link has been used to establish a communication between the matlab-based open source power flow library MATPOWER [13] and the API. This allows the execution of newton power flow and optimal power flow with MATPOWER [13] and the visualization of the obtained results using **SAInt-GUI**.

A **SAInt** project is divided into a static network model, which includes all topological and static properties of the network and a scenario, which is the definition of a case study to be performed on the static network models. The following simulation models are currently implemented in **SAInt**:

1. Steady state gas flow simulation
2. Transient gas flow simulation
3. Steady state AC-Power Flow (AC-PF) simulation (using distributed slack bus algorithm)
4. Steady state AC-Optimal Power Flow (AC-OPF) simulation using a link to MATPOWER [13]
5. Combined steady state gas and steady state AC-PF simulation (with distributed slack bus algorithm)
6. Combined transient gas and steady state AC-PF simulation (using distributed slack bus algorithm)

In the following, we apply **SAInt** for a case study on the Bulgarian and Greek gas and electric transmission system. The topology and basic properties of both networks are depicted in Figures 7 & 8. The networks are interconnected through 14 gas fired power plants (7 located in the south of Greece), two electric driven compressor stations (CS.1 & CS.3, both located in Bulgaria) and one LNG Terminal (located in the south of Greece).

Generation Bus	K_i	η_T
GEN.97	0.121	0.4
GEN.98	0.121	0.45
GEN.116	0.121	0.3
GEN.136	0.061	0.57
GEN.144	0.061	0.45
GEN.152	0.121	0.46
GEN.153	0.121	0.46
GEN.154	0.121	0.55
GEN.155	0.091	0.45
GEN.156	0.061	0.41

Table 7: Participation factors and thermal efficiency assigned to generation buses connected to GPPs

For the case study, we increase the interconnection between both models by assuming five additional compressor stations are powered by electric driven compressors (CS.2, CS.7, CS.8,

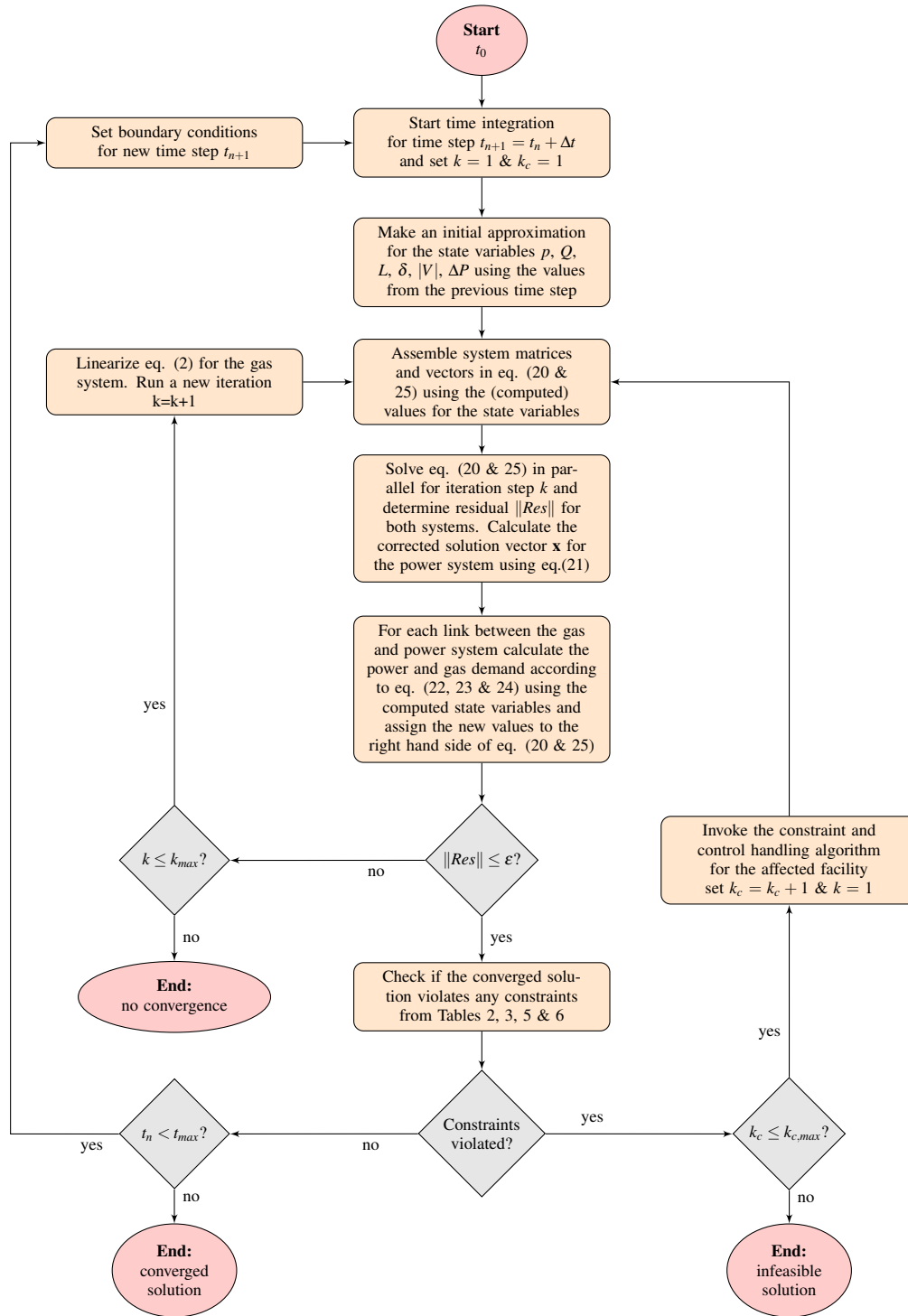


Figure 6: Flow chart for the combined simulation

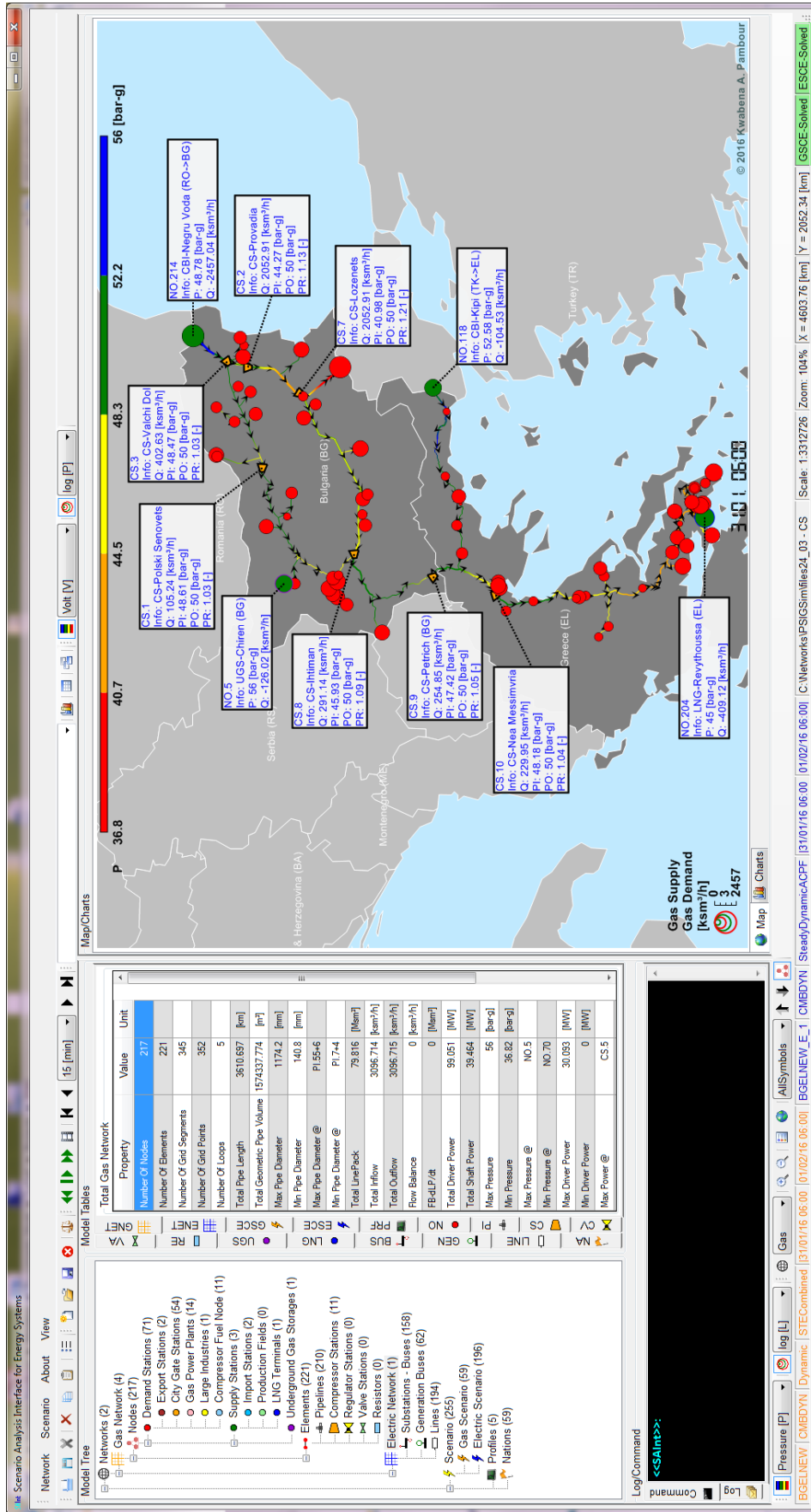


Figure 7: Model of the Bulgarian-Greek gas transmission system plotted in the graphical user interface of SAInt. Map shows results of a steady state computation for the coupled system. Diameter of the circles representing demand (red) and supply (green) nodes correspond to the magnitude of the steady state loads in logarithmic scale, as can be seen from the legend in the bottom left corner. Colors of the pipe elements correspond to the pressure levels indicated in the color bar on top. Pipe arrows indicate gas flow direction. Labels describe a selected number of characteristic facilities in the gas system.

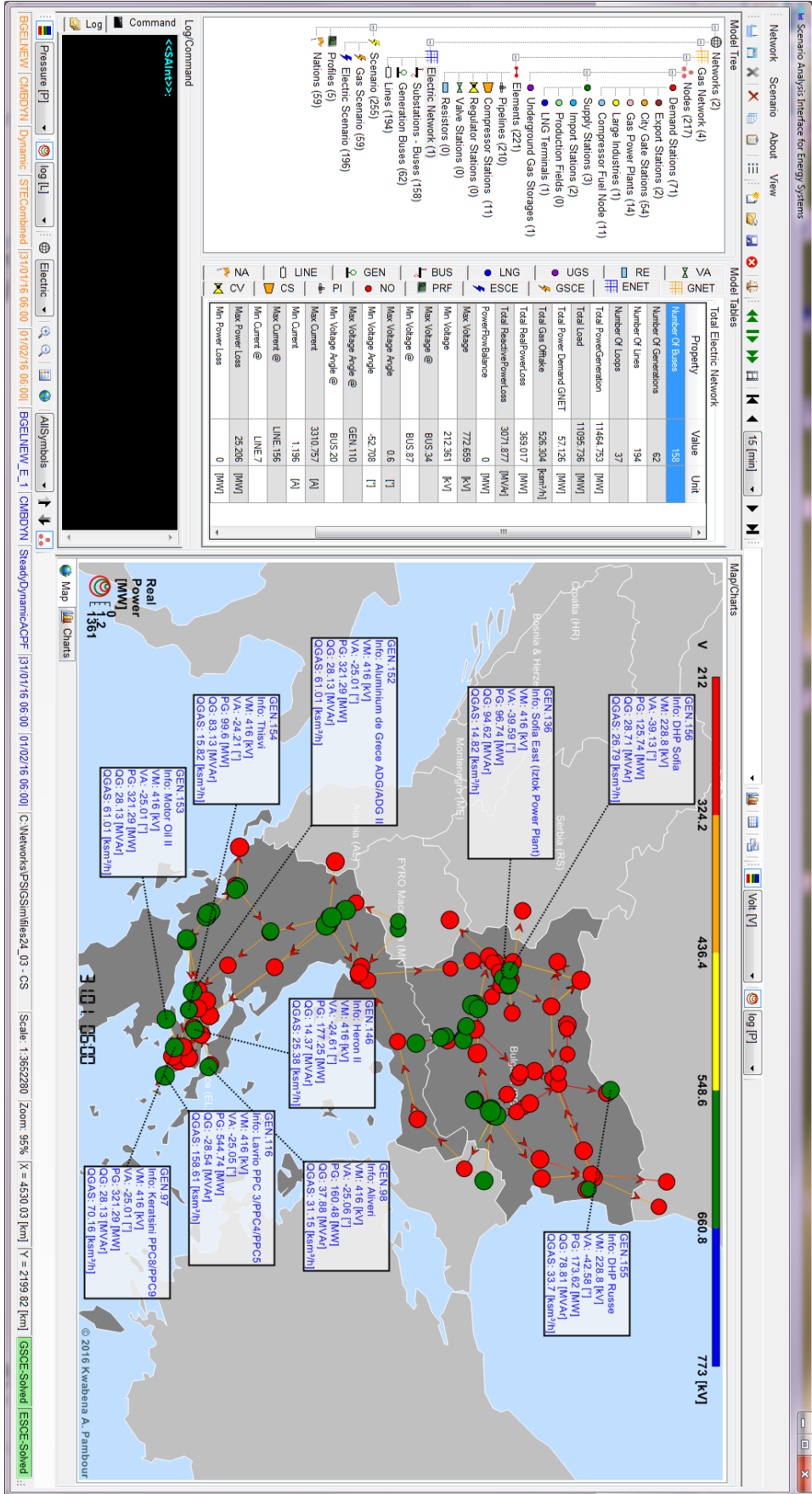


Figure 8: Model of the Bulgarian-Greek power transmission system plotted in the graphical user interface of SAInt. Map shows results of a steady state computation for the coupled system. Diameter of the circles representing load (red) and generation (green) buses correspond to the magnitude of active power in logarithmic scale, as can be seen from the legend in the bottom left corner. Colors of the line elements correspond to the voltage levels indicated in the color bar on top. Transmission line arrows indicate flow direction of electric current. Labels describe a selected number of generation buses (green circles) connected to gas fired power plants.

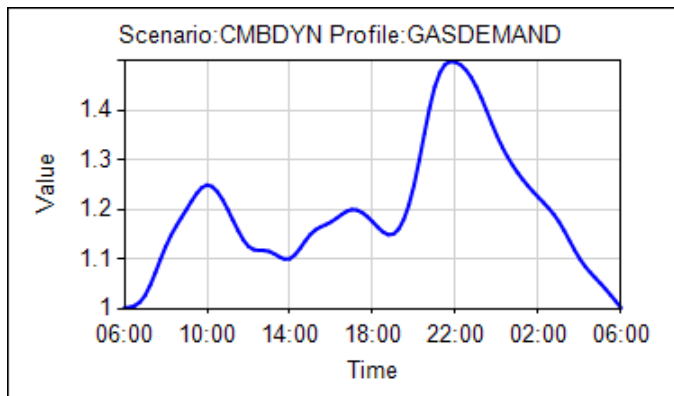


Figure 9: Load profile assigned to city gate stations

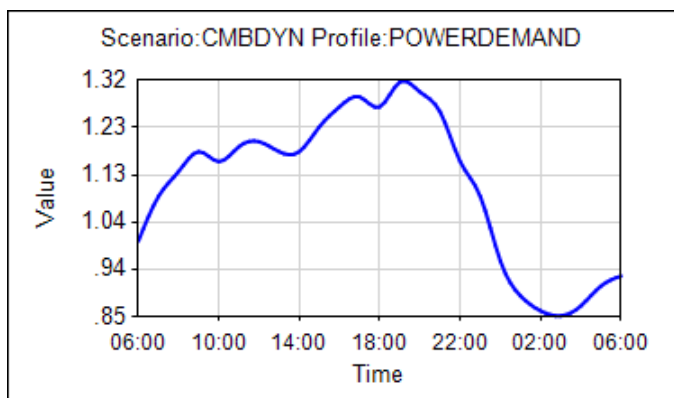


Figure 10: Load profile assigned to load buses

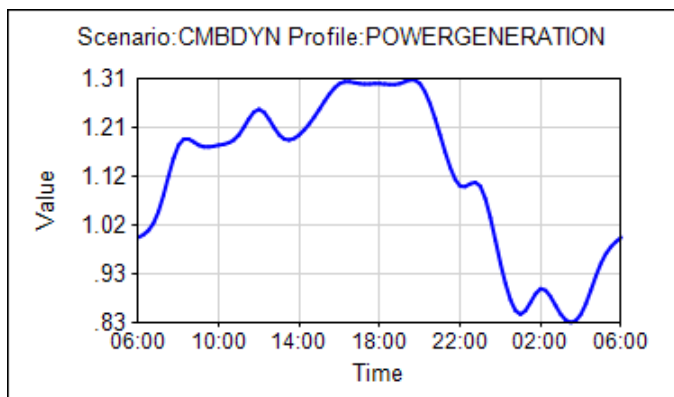


Figure 11: Profile assigned to generation buses

CS.9 & CS.10). The dynamic simulation of the combined model is initiated from the steady state solution shown in Figures 7 & 8 using the load profile from Figure 9 for all city gate stations, the profiles shown in Figures 10 & 11 for all load and generation buses, respectively, and the simulation and gas prop-

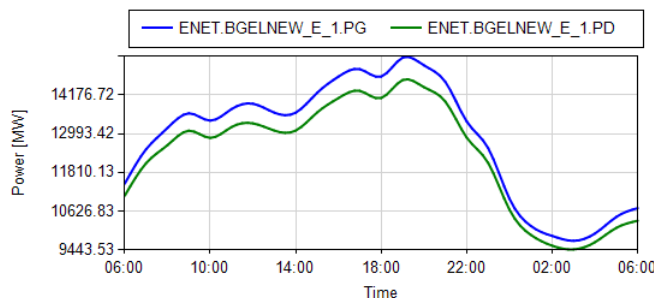


Figure 12: Time series of total power generation (blue) and total power demand (green) for the combined simulation

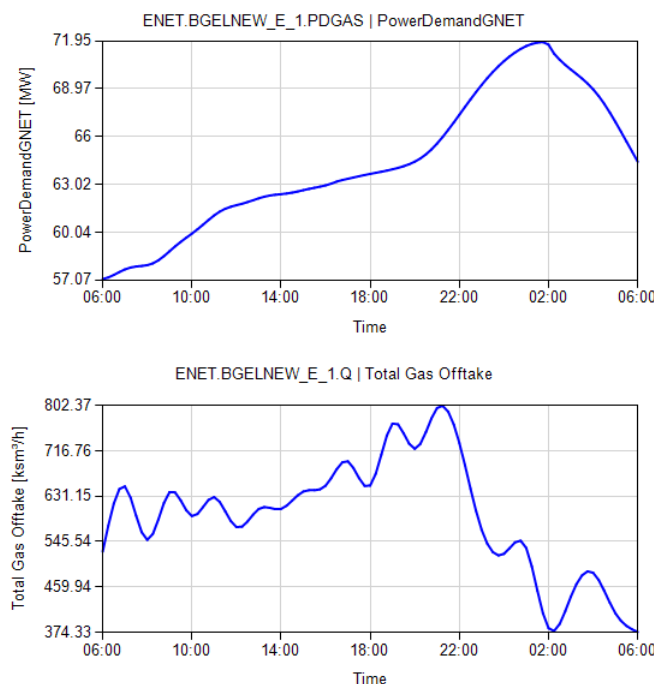


Figure 13: Time series of total power offtake of electric driven compressors stations and LNG terminals (top) and total gas off-take (bottom) of gas power plants for the combined simulation

erties listed in Table 8. Furthermore, we assign to a number of gas power plants connected to generation buses a participation factor K_i and the thermal efficiency listed in Table 7. Thus, these generation units are expected to regulate their active power injections to balance the power system. In addition, we consider the electric power offtake for operating the LNG Terminal Revythoussa located in the south of Greece. Moreover, we assign an outlet pressure control ranging between 40-54 [barg] (580-783 [psig]) to all compressor stations in the gas system. Simulation results are illustrated in Figures 12 - 17 and

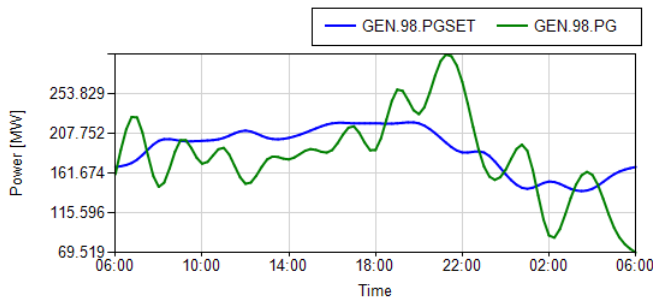


Figure 14: Time series of active power generation set point (blue) and resulting power generation (green) for generation unit GEN.98 in the combined simulation

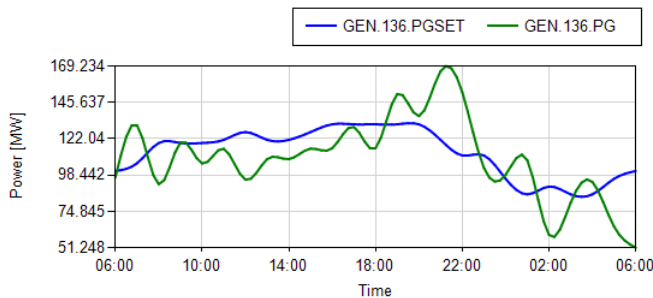


Figure 15: Time series of active power generation set point (blue) and resulting power generation (green) for generation unit GEN.136 in the combined simulation

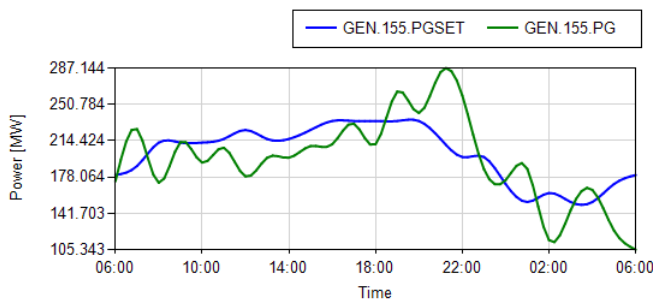


Figure 16: Time series of active power generation set point (blue) and resulting power generation (green) for generation unit GEN.155 in the combined simulation

are discussed in the following.

Figure 12 shows the time evolution of the total active power generation and total power offtake. As can be seen, the shape of both curves is similar to the profile assigned to load buses (s. Fig. 10). The difference between the total power generation and total load curve is equal to the total power loss of

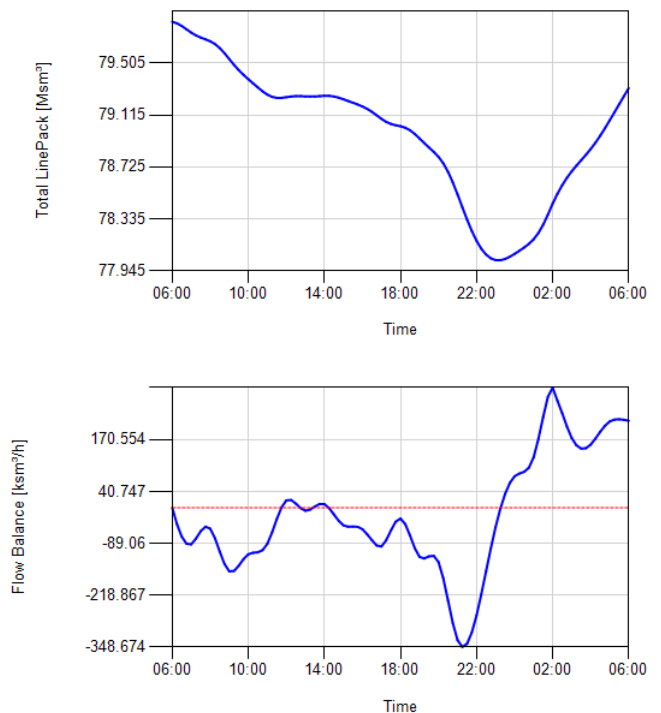


Figure 17: Time series of total line pack (top) and total flow balance (bottom, sum of inflow minus sum of outflow) for the gas system in the combined simulation

the power system, which is caused by the resistances of the transmission lines. The electric power offtake of the gas grid increases right from the start of the simulation and reaches its maximum around 2:00 (s Fig. 13, top). This increase is a result of the overall increase in gas offtake from CGS and GPPs compared to the steady state loads, as can be seen in the time evolution of the flow balance and line pack shown in Figure 17. The compressor stations require more driver power to maintain their outlet pressure set point. However, the power offtake of the gas grid is marginal compared to the total load of the power system. (s Fig. 13, top). The total gas offtake of the GPP units shows larger fluctuations than the assigned generation profile (s. Fig. 13, bottom), because of the assigned participation factors to the GPP units. The GPP units regulate their power generation to balance power demand and losses (s. Fig. 14- 16).

CONCLUSION

In this paper, we presented an integrated simulation tool for a coupled simulation of gas and power systems taking into account the characteristics, the control and constraints of both systems. The integrated model consists of a transient model for the gas system and a steady state AC-Power flow model for the power system, using a distributed slack bus approach for

balancing power demand and power losses. The accuracy of the transient gas model was confirmed by benchmarking simulation results against the commercial software SIMONE. The model of the individual systems were coupled through coupling equations describing the power offtake from electric driven compressor stations and LNG Terminals installed in the gas system and connected to buses of the power network, and the gas offtake for electric power generation in gas fired power plants connected to the gas transport system. The resulting system of equations describing the state change of the combined system between two consecutive time steps is solved iteratively by adapting the boundary conditions expressed by the coupling equations at each iteration step. The algorithm was implemented in an integrated simulation tool **SAInt** and the value of the tool was demonstrated in a case study on an actual combined gas and electric power system of an European region.

In the coming future, we intend to extend the simulation tool to allow the simulation of disruptions and the possibility to define mitigation strategies. By doing this, we intend, to assess how these strategies may reduce the impact of disruptions on both systems.

ACKNOWLEDGMENT

We extend our gratitude to our colleague Dr. Nicola Zaccarelli from the Joint Research Centre - Institute for Energy and Transport, in Petten, Netherlands, for providing the GIS-Data for the presented gas and electric model. We would also like to thank Dr. Tom van der Hoeven for providing the LaTeX template and for the productive discussions and suggestions, which has significantly improved the presented simulation tool.

REFERENCES

- [1] European Union, "Regulation (EU) No 994/2010 of the european parliament and the council of 20 october 2010 concerning measures to safeguard security of gas supply and repealing council directive 2004/67/ec," *Official Journal of the European Union*, 2010, <http://eur-lex.europa.eu/legal-content/EN/TXT/PDF/?uri=CELEX:32010R0994&from=EN>, April 5, 2016.
- [2] B. C. Erdener, K. A. Pambour, R. B. Lavin, and B. Dengiz, "An integrated simulation model for analysing electricity and gas systems," *International Journal of Electrical Power & Energy Systems*, vol. 61, no. 0, pp. 410 – 420, 2014.
- [3] K. A. Pambour, R. Bolado-Lavin, and G. P. Dijkema, "An integrated transient model for simulating the operation of natural gas transport systems," *Journal of Natural Gas Science and Engineering*, vol. 28, pp. 672 – 690, 2016.
- [4] T. van der Hoeven, "Gas transport pipe," No. PSIG 0710, Pipeline Simulation Interest Group, 2007.
- [5] T. van der Hoeven, *Math in Gas and the art of linearization*. Energy Delta Institute, April 2004.
- [6] A. J. Osiadacz, *Simulation and Analysis of Gas Networks*. E. & F.N. SPON, 1987.
- [7] J. D. Glover, M. S. Sarmar, and T. J. Overbye, *Power Systems and Analysis Design*. Global Engineering, fifth ed., 2010.
- [8] G. Andersson, "Modelling and analysis of electric power systems." Lecture 227-0526-00, ITET ETH Zurich, September 2008.
- [9] S. Tong, M. Kleinberg, and K. Miu, "A distributed slack bus model and its impact on distribution system application techniques," *IEEE*, 2005.
- [10] S. Tong, *Slack Bus Modeling for Distributed Generation and Its Impacts on Distribution System Analysis, Operation and Planning*. PhD thesis, Drexel University, 2006.
- [11] A. Martinez-Mares and C. R. Fuerte-Esquivel, "A unified gas and power flow analysis in natural gas and electricity coupled networks," *IEEE Transactions on Power Systems*, vol. 27, November 2012.
- [12] S. A. . Soman, S. A. Khaparde, and S. Pandit, *Computational Methods for Large Sparse Power Systems Analysis*. Springer, 2002.
- [13] R. D. Zimmerman, C. E. Murillo-Sanchez, and R. J. Thomas, "Matpower: Steady-state operations, planning and analysis tools for power systems research and education," *Power Systems, IEEE Transactions*, vol. 26, pp. 12–19, February 2011.

AUTHOR BIOGRAPHY

Kwabena Addo Pambour was born in Accra, Ghana, and grew up in the city of Essen, Germany. He studied Mechanical Engineering and Business Administration at RWTH Aachen University in Germany. In 2010 and 2011 he graduated with a Master of Science (Dipl.-Ing.) in Engineering and a Master of Business Administration (Dipl.-Wirt.-Ing.), respectively. After his studies, he was employed by the European Commission (EC) - Joint Research Centre (JRC) Institute for Energy and Transport (IET) in Petten, Netherlands, as a scientific researcher to conduct research in the area of security of energy supply. Since July 2014, he works as a Customer Support Engineer for the gas software company LIWACOM, situated in Essen, Germany. Mr. Pambour is currently developing his PhD thesis at University of Groningen, Netherlands, where he is inscribed as an external PhD Researcher since December 2014. He has expertise in modeling and simulation of energy systems and in software development. He is the developer of the simulation software SAInt, which is currently used by the European Commission to assess critical energy infrastructures in terms of security of supply.

Dr. Burcin Cakir Erdener was born in Ankara, Turkey, in 1981. She received a B.Sc. degree in Industrial Engineering from Gazi University, Ankara, Turkey, in 2002 and a M.Sc. and Ph.D. in Industrial Engineering from Gazi University, Ankara, Turkey, in 2006 and 2014, respectively. In 2006, she joined the Department of Industrial Engineering, Baskent University, Ankara, as a research assistant. In 2012, she worked in a project for European Commission Joint Research Centre Institute for Energy and Transport, Petten, The Netherlands for one year. Since December 2013, she has been working for European Commission Joint Research Centre Institute for Energy and Transport, Ispra, Italy as a post-doctoral researcher. Her current research interest includes analysis of networks of critical infrastructures including reliability and security analysis of the networks and interactions between different critical infrastructures.

Dr. Ricardo Bolado-Lavin holds a BS in Physics (Complutense University of Madrid, 1987), a Diploma in Nuclear Engineering (CIEMAT, 600-hour course, 1988), and a PhD (Technical University of Madrid, 2004). Since 2010 Dr. Bolado leads the Security of Gas Supply group within the Energy Security, Systems and Market Unit of the Institute for Energy and Transport of the European Commission (DG-JRC). Within this group, he has led the development of hydraulic models for the EU gas transport network to analyze security of gas supply scenarios. Dr. Bolado is the PhD co-director of Mr. Pambour. Before working in the Security of Gas Supply area, he worked in the area of Probabilistic Safety Assessment for High Level Radioactive Waste Repositories and Nuclear Power Plants. He developed these activities at the Institute for Energy and Transport and at the Technical University of Madrid.

Prof. Dr. Gerard P. J. Dijkema is a full professor at University of Groningen since August 2014. He studied Chemical Engineering at University of Twente and acquired his PhD in Engineering Sciences from Delft University of Technology in 2004. Prof. Dijkema is the PhD director of Mr. Pambour. His research interests revolve around modeling the evolution of energy infrastructures and industrial networks as socio-technical systems.

APPENDIX

Parameter	Symbol	Value	Unit
time step	Δt	900	[s]
total simulation time	t_{max}	24	[h]
gas temperature	T	288.15	[K]
dynamic viscosity	η	$1.1 \cdot 10^{-5}$	[kg/m · s]
pipe roughness	k	0.012	[mm]
standard pressure	p_n	1.01325	[bar]
standard temperature	T_n	273.15	[K]
relative density	d	0.6	[-]
calorific value	CV	41.215	[MJ/sm ³]

Table 8: Input parameter for the dynamic simulation of the sample network and the combined model

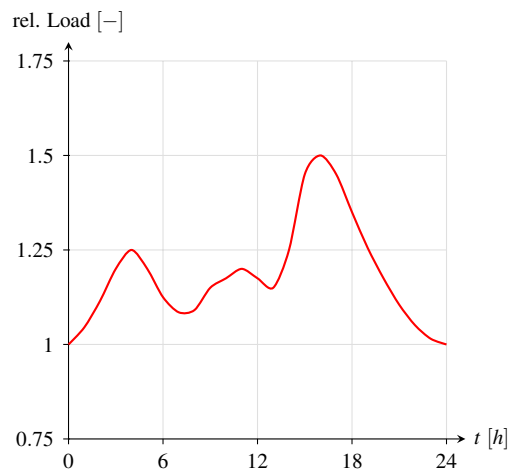


Figure 18: Relative Load profile assigned to demand nodes of the sample network

Pipe	Node		L [m]	D [m]	Node	QSET [ksm^3/s]	PSET [bar-g]
	inlet	outlet					
1	1	2	24000	0.7	1	-	50 (supply)
2	1	3	25000	0.7	2	90	-
3	1	4	20000	0.7	3	29	-
4	4	3	30000	0.7	4	75	-
5	3	2	40000	0.7	5	0	-
6	2	22	45000	0.7	6	55	-
7	2	5	70000	0.6	7	85	-
8	5	6	60000	0.6	8	28	-
9	22	21	52000	0.7	9	90	-
10	6	21	30000	0.6	10	41	-
11	4	10	40000	0.7	11	39	-
12	4	11	35000	0.6	12	20	-
13	4	12	25000	0.7	13	0	-
14	12	13	70000	0.6	14	80	-
15	12	11	30000	0.7	15	45	-
16	11	10	50000	0.6	16	0	-
17	13	14	60000	0.6	17	120	-
18	10	14	100000	0.6	18	42	-
19	14	15	80000	0.7	19	18	-
20	10	9	75000	0.6	20	35	-
21	15	9	80000	0.7	21	29	-
22	15	16	75000	0.6	22	71	-
23	16	17	80000	0.7	23	0	-
24	10	6	40000	0.6	24	0	-
25	9	17	65000	0.7	25	0	-
26	9	8	40000	0.6	Compressor	POSET [bar-g]	
27	8	17	55000	0.6	1	55	
28	9	7	45000	0.6	2	55	
29	8	18	30000	0.7	3	55	
30	7	18	42000	0.6			
31	6	7	20000	0.7			
32	18	19	30000	0.6			
33	7	20	40000	0.7			
34	20	19	32000	0.6			
35	20	21	45000	0.7			

Table 9: Input data for the reference network taken from [6]